Separation Science and Technology
Publication details, including instructions for authors and subscription information:
http://www.informaworld.com/smpp/title~content=t713708471

Gradient Hydroxyapatite Chromatography with Small Sample Loads. VI. Effect of Thermal Brownian Diffusion Plus Diffusion Due to the Second Type of Flow Heterogeneity Occurring near the Top of the Column

Tsutomu Kawasaki[a]
[a] LABORATOIRE DE GENETIQUE MOLECULAIRE INSTITUT DE RECHERCHE EN BIOLOGIE MOLECULAIRE FACULTE DES SCIENCES, PARIS, FRANCE

To cite this Article Kawasaki, Tsutomu(1982) 'Gradient Hydroxyapatite Chromatography with Small Sample Loads. VI. Effect of Thermal Brownian Diffusion Plus Diffusion Due to the Second Type of Flow Heterogeneity Occurring near the Top of the Column', Separation Science and Technology, 17: 2, 337 — 357
To link to this Article: DOI: 10.1080/01496398208068543
URL: http://dx.doi.org/10.1080/01496398208068543

SEPARATION SCIENCE AND TECHNOLOGY, 17(2), pp. 337-357, 1982

Gradient Hydroxyapatite Chromatography with Small Sample Loads. VI. Effect of Thermal Brownian Diffusion Plus Diffusion Due to the Second Type of Flow Heterogeneity Occurring near the Top of the Column

TSUTOMU KAWASAKI

LABORATOIRE DE GENETIQUE MOLECULAIRE
INSTITUT DE RECHERCHE EN BIOLOGIE MOLECULAIRE
FACULTE DES SCIENCES
PARIS 5, FRANCE

Abstract

A theory of gradient hydroxyapatite chromatography with small sample loads is developed by taking into account the associated effect of thermal Brownian diffusion plus diffusion due to the second type of flow heterogeneity occurring near the top of the column. Theoretical chromatograms with slightly asymmetrical shapes similar to those obtained experimentally can be calculated. However, this effect is small. The earlier theory in which the effect is assumed to be infinitesimal is valid from a practical point of view. The possibility of drastically increasing the chromatographic resolution is suggested.

INTRODUCTION

Earlier in this series (*1–5*), in Part V (*5*), a theory of gradient hydroxyapatite (HA) chromatography with small sample loads was developed by taking into account the effect of the top of the column.

At least with HA chromatography the total longitudinal diffusions in the column are classificable into three types: thermal Brownian diffusion and two types of diffusions provoked by two types of flow heterogeneities occurring in the column (*6*). Thus, let us divide the column into a number of parallel hypothetical columns with diameters of the order of magnitude of the interdistances among crystals packed in the total column. It can be assumed that, due to the heterogeneity in interstices among the crystals being packed, the flow rate of the solution fluctuates at random not only among different

longitudinal positions on the same microcolumn but also among parts of different microcolumns existing within the same vertical section of the total column. The flow heterogeneity occurring due to this mechanism is called as the first type (*6*). Due to a viscous property of the solution, however, it might be possible that the flow rate in a interstice in the column depends upon the distance from the crystal surface. Therefore, even within a microcolumn, a flow heterogeneity is realizable; this is called the second type of flow heterogeneity (*6*). It can be assumed, however, that the effect of the second type of flow heterogeneity, if it occurs, is so small that it does not provoke the heterogeneity in molecular density in the interstice between the crystals (*6*). Nevertheless, the movement of the molecules in a interstice in the column would, in general, be disturbed by the second type of flow heterogeneity (*6*). Under this assumption, it is impossible to distinguish chromatographically the molecular diffusion occurring caused by the second type of flow heterogeneity from thermal Brownian diffusion; the effect of Brownian diffusion plus diffusion due to the second type of flow heterogeneity (briefly B-dif. plus STFH-dif.; see Ref. 5) behaves as an element of the chromatographic mechanism (*6*).

The effect of the column top is conceivable only in terms of the B-dif. plus STFH-dif. effect occurring near the top of the column (*5, 6*). In Ref. 5 the extreme case occurring at the limit when the B-dif. plus STFH-dif. effect tends to zero was considered; under this situation, diffusion due to the first type of flow heterogeneity is the only longitudinal diffusion that is realizable in the column. In the theory in Refs. *1–4* also, the B-dif. plus STFH-dif. effect is assumed to be infinitesimal [cf. both Remark (3) in the Introduction Section in Ref. 5 and Remark (2) in Theoretical Section A in Ref. *6*]. The purpose of the present work is to develop a theory in which account is taken of the finite effect of B-dif. plus STFH-dif. For this purpose it is first necessary to reduce the fundamental continuity equation of gradient chromatography (originally derived as Eq. 17 in Ref. *3* and reproduced as Eq. A-1 in the Appendix) to a simpler form (Eq. 7). Theoretical chromatograms with slightly asymmetrical shapes similar to those obtained experimentally (with a slower decrease in height on the right-hand side of the pattern than on the other side; see Ref. *2*) can be calculated. It can be concluded, however, that the B-dif. plus STFH-dif. effect is small; the earlier theory (*1–5*) is valid from a practical point of view.

THEORETICAL

A. Approximate Form of the Fundamental Continuity Equation for Gradient Chromatography

In Ref. *3* a fundamental continuity equation for gradient chromatography was derived [Eq. 17 in Ref. *3* (or Eq. 1 in Ref. 5); reproduced as Eq. A-1 in

the Appendix], and the initial boundary condition of this equation was represented in terms of a delta function [Eq. 74 in Ref. *3* (or Eq. 9 in Ref. 5)] which can be rewritten into a more explicit form (Eq. 17 in Ref. 5), i.e.,

$$C(s = +0, m) = \delta(m - m_{in}) \tag{1}$$

Brief explanations for any symbols involved in the equations (except those which are defined by the equations themselves) are given at the end of the paper. (For the symbol s in Eq. 1, see Eq. 3.) By solving the fundamental chromatographic equation (Eq. A-1 in the Appendix) under the boundary condition given by Eq. (1), a theoretical chromatogram represented by both Eqs. (62) and (73) in Ref. *3* (or Eqs. 12 and 6 in Ref. 5) can be obtained. In Ref. 5 a new interpretation was given to these equations, taking into account the effect of the top of the column. However, provided the molarity range over which a chromatogram appears is small around the mean elution molarity, Eqs. (62) and (73) in Ref. *3* (or Eqs. 12 and 6 in Ref. 5) reduce to a single equation with a Gaussian form [Eq. 8 in Ref. *4* (or Eq. 28 in Ref. 5)]. This equation can be rewritten as

$$C(s, m) = \frac{1}{\sqrt{2\pi}\sigma(s)} e^{-\frac{[m-\mu(s)]^2}{2[\sigma(s)]^2}} \tag{2}$$

where

$$s = gL \tag{3}$$

$$\mu(s) = \frac{1}{\varphi'}\{[(x' + 1)\varphi' q s + (\varphi' m_{in} + 1)^{x'+1}]^{\frac{1}{x'+1}} - 1\} \tag{4}$$

$$\sigma(s) = \frac{\sqrt{2g\theta_0 s}}{\bar{B}(s)} \tag{5}$$

and

$$\bar{B}(s) \equiv B_\lambda[\mu(s)] = \frac{1}{1 + q[\varphi'\mu(s) + 1]^{-x'}} \tag{6}$$

It can be confirmed that Eq. (2), in fact, reduces to Eq. (1) at the limit when s tends to $+0$, since μ (Eq. 4) and σ (Eq. 5) tend to $m_{in} + 0$ and $+0$, respectively.

In the Appendix a partial differential equation

$$g\theta_0 \frac{d}{ds}\left\{\frac{s}{[\bar{B}(s)]^2}\right\} \frac{\partial^2 C}{\partial m^2} = \frac{1 - \bar{B}(s)}{\bar{B}(s)} \frac{\partial C}{\partial m} + \frac{\partial C}{\partial s} \tag{7}$$

is derived from which Eq. (2) can be generated as a solution under the initial boundary condition given by Eq. (1). It can be considered that Eq. (7) is an approximate form of Eq. (A-1) (for details, see the Appendix). It is important to note that, under a more general boundary condition:

$$C(s = +0, m) = C_0(m) \tag{8}$$

Equation (7) has a solution

$$C(s, m) = \frac{1}{\sqrt{2\pi}\sigma(s)} \int_{-\infty}^{\infty} C_0(m') e^{-\frac{|m-m'+m_{in}-\mu(s)|^2}{2|\sigma(s)|^2}} dm' \tag{9}$$

(cf. Eq. A-11 in the Appendix). It can be confirmed that, if $C_0(m')$ reduces to the delta function (Eq. 1), then Eq. (9) reduces to Eq. (2).

B. Theoretical Chromatogram under the Effect of Brownian Diffusion Plus Diffusion Due to the Second Type of Flow Heterogeneity Occurring Near the Top of the Column

Within a small width

$$\Delta L = 4\hat{\theta}_0 \tag{10}$$

near the top of the column, the effect of the first type of flow heterogeneity (see Introduction Section) is negligible and molecules are performing random motions receiving the B-dif. plus STFH-dif. effect (*5*, *6*). We consider below the case of small sample loads (1) when the width in the initial molecular band at the column top is smaller than, or equal to, ΔL, and (2) when the partition, B, of molecules in solution occurring in any column section within ΔL is very small. The latter is a necessary condition for molecules to be initially retained on the column (*5*, *6*).

Introducing a new parameter

$$s' = s + 4g\hat{\theta}_0 \tag{11}$$

Eq. (9) can be rewritten as

$$C(s, m) = C(s' - 4g\hat{\theta}_0, m)$$

$$= \frac{1}{\sqrt{2\pi}\sigma(s' - 4g\hat{\theta}_0)} \int_{-\infty}^{\infty} C_0(m') e^{-\frac{|m-m'+m_{in}-\mu(s'-4g\hat{\theta}_0)|^2}{2|\sigma(s'-4g\hat{\theta}_0)|^2}} dm' \tag{9'}$$

The reason why Eq. (9) has been rewritten as Eq. (9′) will be understood later. Based on the second point of view on gradient chromatography (*3*, 5), Eq. (9) or (9′) is simply representing the molecular distribution in the abstract flux migrating on the abstract m-coordinate system. s is proportional to time t provided the flow rate is constant with respect to t (*3*, 5). From the first point of view (*3*, 5), however, s is proportional to the longitudinal distance L from the top of the column (see Eq. 3). m represents the molarity of competing ions in solution at column position L. If the position L coincides with the bottom of the column, m is the molarity of the ions in solution that have just been eluted out of the column (*3*, 5). $m - m_{in}$, therefore, is proportional to time t provided the flow rate is constant with respect to t (*3*, 5).

Let us consider the part $L > 4\hat{\theta}_0$ of the total column as a subcolumn. The top of the subcolumn therefore coincides with position $L = 4\hat{\theta}_0$ of the total column. Let us also consider that s is the parameter that is concerned with the subcolumn. Based on the first point of view under this consideration, s should be defined, instead of as in Eq. (3), as

$$s = g(L - 4\hat{\theta}_0) \tag{12}$$

where L is still the distance from the top of the total column. It is therefore s' (Eq. 11) that now is proportional to L, which leads to the relationship

$$s' = gL \tag{13}$$

From the second point of view, however, it is s (defined by Eq. 12), and not s' that is proportional to t.

At position $L = 4\hat{\theta}_0$ on the total column or the top of the subcolumn [where $s' = 4g\hat{\theta}_0$ (Eq. 13) and $s = 0$ (Eq. 12)], a relationship given by Eq. (27) in Ref. 5 is fulfilled. In the second point of view, Eq. (27) in Ref. 5, therefore represents the initial distribution $C_0(m)$ (Eq. 8) in the abstract flux *concerning the subcolumn* and occurring at time 0 when $s = 0$. We can therefore write

$$\left.\begin{aligned} C_0(m) &= \frac{1}{4g\hat{\theta}_0}\frac{dr(m)}{dm}e^{-\frac{r(m)}{4g\hat{\theta}_0}} && (\text{for } m \geq m_{in}) \\ &= 0 && (\text{for } m < m_{in}) \end{aligned}\right\} \tag{14}$$

where $r(m)$ is defined by Eq. (A-19) in the Appendix as

$$r(m) = \int_{m_{in}}^{m} \frac{B_\lambda(m')}{1 - B_\lambda(m')}\, dm' \tag{15}$$

[cf. Remark (1) below].

The theoretical chromatogram for the column with length $L \geq 4\hat{\theta}_0$ or $s' \geq 4g\hat{\theta}_0$ can be calculated if Eq. (14) is substituted into Eq. (9'). It should be emphasized that the chromatogram is a concept that is concerned with the total column and not with the subcolumn. Further, the chromatogram itself is conceivable only from the first point of view (*3, 5*). Therefore, let us represent a chromatogram by $C'(s', m)$ instead of by $C(s' - 4g\hat{\theta}_0, m)$ (cf. Eq. 9'). $C'(s', m)$ (when $s' \geq 4g\hat{\theta}_0$) can now be written as

$$\begin{aligned} C'(s' \geq 4g\hat{\theta}_0, m) &= \frac{1}{\sqrt{2\pi}\sigma(s' - 4g\hat{\theta}_0)} \int_{m_{in}}^{\infty} \frac{1}{4g\hat{\theta}_0} \frac{dr(m')}{dm'} \\ &\quad \times e^{\frac{r(m')}{4g\hat{\theta}_0} - \frac{[m - m' + m_{in} - \mu(s' - 4g\hat{\theta}_0)]^2}{2[\sigma(s' - 4g\hat{\theta}_0)]^2}} \\ &= \frac{1}{\sqrt{2\pi}\sigma(s' - 4g\hat{\theta}_0)} \\ &\quad \int_0^{\infty} e^{-\left\{\rho - \frac{[m + m_{in} - \mu(4g\hat{\theta}_0\rho) - \mu(s' - 4g\hat{\theta}_0)]^2}{2[\sigma(s' - 4g\hat{\theta}_0)]^2}\right\}} d\rho \end{aligned} \tag{16}$$

where the second equality has been obtained from both substitution of $\rho = r(m')/(4g\hat{\theta}_0)$ and consideration of the fact that, generally if $r(\mu') = s$, then $\mu' = \mu(s)$ (cf. Eqs. A-18 and A-20 in the Appendix). This means that if $r(m') = 4g\hat{\theta}_0\rho$, then $m' = \mu(4g\hat{\theta}_0\rho)$.

It should be noted that the function $C'(s', m)$ calculated from Eq. (16) takes finite values even when $m < m_{in}$, whereas the chromatogram should actually appear only in the molarity range of $m \geq m_{in}$. This inconsistency arises from the fact that Eq. (16) has been derived by using both the first and second equalities in Eq. (14) whereas it is only the first one that involves the physical meaning and the second equality has been added only for convenience sake [see the explanation of Eq. 27 in Ref. 5 that corresponds to Eq. 14; cf. Remark (1) below]. As in Ref. 5, an interpretation should now be introduced that, in Eq. (16), it is only the part $m \geq m_{in}$ of C' that has the physical meaning. The other part, $m < m_{in}$, that formally occurs in Eq. (16) actually should occur at the beginning, $m = m_{in}$, of the molarity gradient forming a sharp peak. The peak gradually disappears in the early stages of the development process [cf. Remark (2) below].

When $0 < L < 4\hat{\theta}_0$ or $0 < s' < 4g\hat{\theta}_0$, then on the basis of a consideration

similar to that used for the derivation of the first equality in Eq. (14) [i.e., the first equality in Eq. 27 in Ref. 5; cf. Remark (1) below], we can derive

$$C'(0 < s' < 4g\hat{\theta}_0, m) = \frac{1}{s} \frac{dr(m)}{dm} e^{-\frac{r(m)}{s}} \tag{17}$$

Remark (1). Equations (14) and (15) can be compared with Eqs. (27) and (26) in Ref. 5, respectively. In the latter two equations, the expression r is used instead of the expression $r(m)$ in the former two. The reason is mentioned in Ref. 5. In Eqs. (14) and (15) the expression $r(m)$ can be used. This is because the concept of local molarity, m_λ (5), does not appear in the approximate chromatographic equation, Eq. (7).

Remark (2). The "development process" on the column is a concept captured from the first point of view on gradient chromatography. "Early stages," therefore, mean chromatographic stages when the longitudinal distance of the mean part of the molecular band migrating on the column to the column top still is small, provided that the length of the column is large enough for the mean part of the band to exist on the column at the instant under consideration. For details, see Ref. 5, Theoretical Section B, for the special case when $\hat{\theta}_0 = 0$ is argued. The argument is valid independent of the value of $\hat{\theta}_0$, however.

Some Numerical Calculations and the Relationship with the Experiment

Equation (12) shows that, among parameters s, g, and L, it is a pair that are independent provided $\hat{\theta}_0$ is given. Experimentally, it is common practice that the pair (g, L) *a priori* is given. The chromatogram C' (Eqs. 16 and 17) is obtained as a function of m. It is therefore convenient first to rewrite Eqs. (16) and (17) into forms in which both parameters g and L are explicitly involved. Calling f as this expression of C', f can be expressed as

$$f(m; g, L \geq 4\hat{\theta}_0) = \frac{1}{\sqrt{2\pi}\sigma(g, L)} \int_0^{\infty} e^{-\left\{\rho + \frac{[m + m_{in} - \mu(4g\hat{\theta}_0\rho) - \mu[g(L - 4\hat{\theta}_0)]]^2}{2[\sigma(g,L)]^2}\right\}} d\rho \tag{18}$$

and

$$f(m; g, 0 < L < 4\hat{\theta}_0) = \frac{1}{gL} \frac{dr(m)}{dm} e^{-\frac{r(m)}{gL}}$$

where

$$\sigma(g, L) = \sqrt{2\theta_0(L - 4\hat{\theta}_0)}\, g\left[1 + \frac{q}{\{\varphi'\mu[g(L - 4\hat{\theta}_0)] + 1\}^{x'}}\right] \quad (19)$$

(cf. Eqs. 4–6 and 12).

The continuous curve in Fig. 1 [reproduced from the left-hand pattern in Fig. 5(b) in Ref. *2*] illustrates a theoretical chromatogram for lysozyme, calculated from both Eqs. (62) and (73) in Ref. *3* (or Eqs. 12 and 6 in Ref. 5); Eq. (62) in Ref. *3* (or Eq. 12 in Ref. 5) represents the solution of Eq. (A-1) in the Appendix (see Theoretical Section A). On the abscissa in Fig. 1, the suffix (K^+) attached to the variable m represents the fact that the competing ions (*1*–5) that constitute the molarity gradient is potassium, and that the m value is concerned with potassium. The same suffix will also appear in Figs. 2–4. For any symbols appearing in text, the suffix (K^+) is omitted for simplicity, however. Now, for calculation in Fig. 1, it is assumed that the B-dif. plus STFH-dif. effect is infinitesimal, i.e., that $\hat{\theta}_0 = 0$ cm (cf. Introduction Section). Provided that $\hat{\theta}_0 \neq 0$ cm, then even the effect of the existence itself of the column top is negligible under the experimental conditions that are applied (for the effect of the existence itself on the column

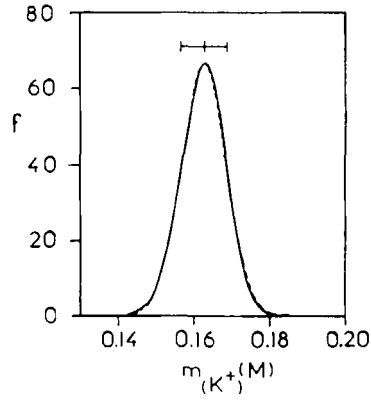

FIG. 1. Continuous curve: Theoretical chromatogram for lysozyme as a function of potassium molarity, $m_{(K^+)}$, calculated from both Eqs. (62) and (73) in Ref. *3* (or Eqs. 12 and 6 in Ref. 5) under the experimental conditions of $L = 55$ cm, $g_{(K^+)} = 4.239 \times 10^{-4} M$/cm, and $m_{in(K^+)} = 0.0015\ M$, where the suffix (K^+) indicates that the parameters are concerned with potassium ions from the buffer. For the calculation it is assumed: $\varphi' = 9\ M^{-1}$, $\hat{\theta}_0 = 0$ cm, $\theta_0 = 0.3$ cm, $x' = 7$, and $\ln q = 6.7$. (Reproduced from the left-hand pattern in Fig. 5 b in Ref. *2*.) Dotted curve: Approximate Gaussian chromatogram, calculated from Eq. (2). The centers of gravity and the lower and upper limits of the chromatographic peaks are shown also; these are essentially the same for the two chromatograms.

top, see Ref. 5). For the other experimental parameters the best values have been used, x' and $\ln q$ characterizing the lysozyme molecule (for detail, see the legend of Fig. 1 and Ref. *2*). The dotted curve in Fig. 1 represents the approximate Gaussian chromatogram calculated from Eq. (2). It can be seen in Fig. 1 that the approximate chromatogram is essentially identical with the chromatogram calculated from the solution of Eq. (A-1) (i.e., Eqs. 62 and 73 in Ref. *3* or Eqs. 12 and 6 in Ref. 5). The corresponding experimental chromatogram is shown in Fig. 6(b) in Ref. *2*. It can be seen in Fig. 6 in Ref. *2*, however, that, in comparison with theoretical chromatograms, experimental chromatograms, in general, are slightly asymmetrical with a slower decrease in height on the right-hand side of the pattern than on the other side.

Figure 2 shows that, if the finite effect of B-dif. plus STFH-dif. is taken into consideration, asymmetrical theoretical chromatograms similar to those obtained experimentally can be calculated. Thus, Figs. 2(a), (b), and (c) illustrate theoretical chromatograms calculated from Eq. (18) by using the value 0.005 cm for the parameter $\hat{\theta}_0$ that measures this effect. The experimental conditions in any part of Fig. 2 are the same as those in Fig. 1 (see above), and the dotted vertical line in any part of Fig. 2 shows the position of the center of gravity of the theoretical chromatogram(s) in Fig. 1. This can be assumed to be a best position (*2*). In Fig. 2(a) the same values are used as in Fig. 1 for the experimental parameters φ', θ_0, x', and $\ln q$. It can be seen in Fig. 2(a), however, that, due to the finite value of $\hat{\theta}_0$ that has been introduced above, the mean position of the chromatogram is slightly displaced to the right in comparison with the case of $\hat{\theta}_0 = 0$ cm (dotted vertical line). The width in the chromatographic peak becomes slightly too large in comparison with a best width (see Fig. 1). A best position of the chromatogram is obtained if a slightly smaller value, 6.6, of $\ln q$ is assumed (Fig. 2b). A best width in the chromatogram can be obtained by using a smaller value, 0.2 cm, of θ_0. Thus a best final chromatogram (under the assumption of $\hat{\theta}_0 = 0.005$ cm) is derived (Fig. 2c). It can be seen in Fig. 2(c) that the chromatogram, in fact, is slightly asymmetrical with a slower decrease in height on the right-hand side of the pattern than on the other side as in the experimental chromatogram (see Fig. 6 in Ref. *2*).

Figures 2(d), (e), and (f) illustrate theoretical chromatograms with $\hat{\theta}_0 = 0.01$ cm that correspond to those in figs. 2(a), (b), and (c), respectively. Thus the values of the experimental parameters that are assumed in Fig. 2(d) are the same as those assumed in both Figs. 2(a) and 1 with $\theta_0 = 0.3$ cm and $\ln q = 6.7$. In Fig. 2(e) a slightly smaller value, 6.5, of $\ln q$ is assumed in order to obtain a best mean position of the chromatographic peak. In Fig. 2(f) a further change in the θ_0 value to 0.1 cm is made to obtain a best width in the chromatogram. By comparing Fig. 2(f) (best theoretical chromatogram attainted under the assumption of $\hat{\theta}_0 = 0.01$ cm), Fig. 2(c) (best chromato-

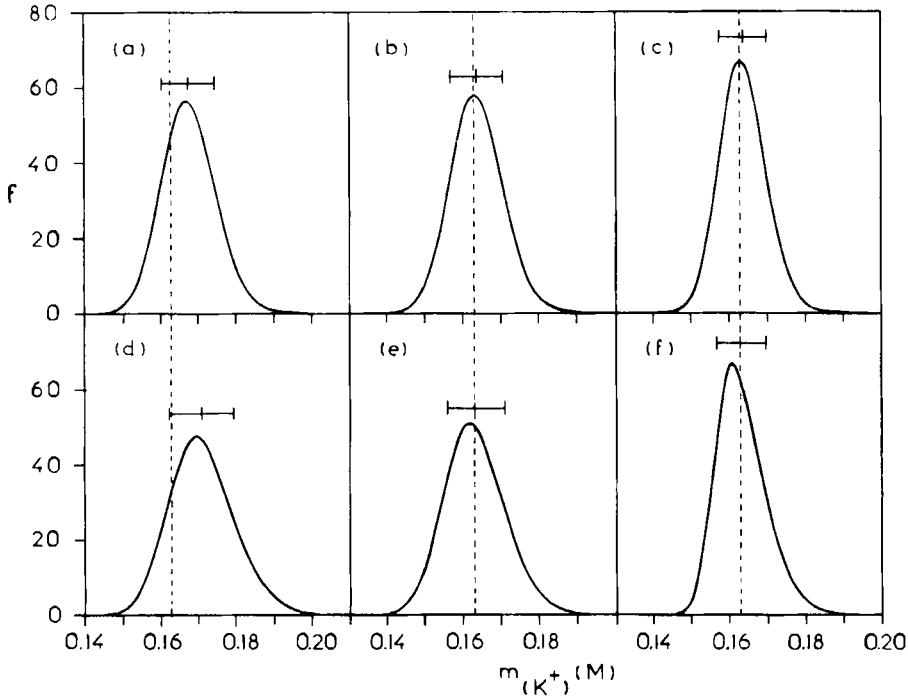

FIG. 2. Theoretical chromatograms for lysozyme as functions of potassium molarity, $m_{(K^+)}$, calculated from Eq. (18) by taking into account the finite effect of B-dif. plus STFH-dif. The centers of gravity and the lower and upper limits of the chromatographic peaks are also shown. The experimental conditions are the same as those in Fig. 1. The dotted vertical lines show the position of the center of gravity of the theoretical peak in Fig. 1, which can be assumed to be a best position. For calculations, it generally is assumed: $\varphi' = 9\ M^{-1}$ and $x' = 7$; these are assumptions common to those involved in Fig. 1. The other assumptions depend upon the parts of the figure with $\hat{\theta}_0 = 0.005$ cm, $\theta_0 = 0.3$ cm, and $\ln q = 6.7$ in (a); $\hat{\theta}_0 = 0.005$ cm, $\theta_0 = 0.3$ cm, and $\ln q = 6.6$ in (b); $\hat{\theta}_0 = 0.005$ cm, $\theta_0 = 0.2$ cm, and $\ln q = 6.6$ in (c); $\hat{\theta}_0 = 0.01$ cm, $\theta = 0.3$ cm, and $\ln q = 6.7$ in (d); $\hat{\theta}_0 = 0.01$ cm, $\theta_0 = 0.3$ cm, and $\ln q = 6.5$ in (e); and $\hat{\theta}_0 = 0.01$ cm, $\theta_0 = 0.1$ cm, and $\ln q = 6.5$ in (f). Parts (c) and (f) are best chromatograms obtained under assumptions of $\hat{\theta}_0 = 0.005$ cm and $\hat{\theta}_0 = 0.01$ cm, respectively. For details, see text.

gram under the assumption of $\hat{\theta}_0 = 0.005$ cm) and Fig. 1 (best chromatogram under the assumption of $\hat{\theta}_0 = 0$ cm), it can be understood that the symmetricity in the chromatographic peak decreases with an increase in the $\hat{\theta}_0$ value. It is difficult, however to estimate the exact $\hat{\theta}_0$ value by comparing the shape of the theoretical chromatograms (Figs. 1, 2c, and 2f) with the experimental result (Fig. 6 in Ref. 2), since the shape of the experimental

chromatogram fluctuates considerably depending upon the experiment. Figure 6 in Ref. *2* shows only typical experimental results.

It can be deduced, however, that the actual $\hat{\theta}_0$ value, at most, is of the order of magnitude of 0.005 cm. Thus points of any part of Fig. 3 are experimental plots of ln s vs elution molarity, m_{elu}, at the center of gravity of lysozyme chromatographic peaks for three different slopes, g, of the potassium molarity gradients that are applied which have been reproduced from Fig. A2 in Ref. *2*, Appendix II. The curve in Fig 3a (also reproduced from Fig. A2 in Ref. *2*, Appendix II) is theoretical, calculated from Eq. (4) on the basis of the assumption of $\hat{\theta}_0 = 0$ cm. The values of the experimental parameters that are used for the calculation are the same as those used in Fig. 1. The curves in both Figs. 3b and 3c are theoretical, calculated from Eq. (18) by taking into account finite $\hat{\theta}_0$ values 0.005 and 0.01 cm, respectively. The values of the experimental parameters that are used for the calculations of Figs. 3b and 3c are the same as those assumed in Figs. 2(c) and (f), respectively. The theoretical curves in Figs. 3b and 3c are virtually independent of the θ_0 value, however. (In Eq. 4, from which the theoretical curve in Fig. 3a has been calculated, the paremeter θ_0 is not involved at all.) It can be seen in Fig. 3 that, if $\hat{\theta}_0 = 0$ cm, the theoretical curve is independent of the slope g of the molarity gradient (part a). If $\hat{\theta}_0$ is finite, however, the curve depends upon the g value. As a result, three theoretical curves are obtained for three different g's that are applied (Figs. 3b and 3c). With an increase in $\hat{\theta}_0$, the split among the three curves becomes more prominent (compare Fig. 3b with Fig. 3c). It is difficult, however, to find in Fig. 3 the dependence of the experimental (m_{elu}, ln s) plot upon g. Taking into account fortuitous fluctuations in the experimental plot, it would be possible to conclude from Fig. 3 that the actual $\hat{\theta}_0$ value is, at most, of the order of magnitude of 0.005 cm.

In Fig. 1 in Ref. *2* are plotted standard deviation of lysozyme experimental chromatograms (corresponding to the experimental points in Fig. 3) vs length L of the column for the three slopes g of the molarity gradient occurring in Fig. 3. The corresponding theoretical curves, calculated from Eqs. (62) and (73) in Ref. *3* (or Eqs. 12 and 6 in Ref. 5; Eq. 62 in Ref. *3*; or Eq. 12 in Ref. 5 is the solution of Eq. A-1 in the Appendix) on the basis of the assumption of $\hat{\theta}_0 = 0$ cm, are also plotted in Fig. 1 in Ref. *2*. The theoretical curves have been calculated from Eq. (18), taking into account the finite $\hat{\theta}_0$ effect. Here, again, good fits with the experiment have been obtained only when $\hat{\theta}_0$ is smaller than or, at most, of the order of magnitude of 0.005 cm.

Finally, Fig. 4 illustrates typical theoretical chromatograms for lysozyme on columns with several small lengths L calculated from Eq. (18). The sharp peak that should appear at $m = m_{in}$ (Theoretical Section B) is not illustrated in the figure except when $L = 4\hat{\theta}_0 = 0.02$ cm (cf. Remark below). Except for the column length, the experimental conditions that are assumed in Fig. 4 are

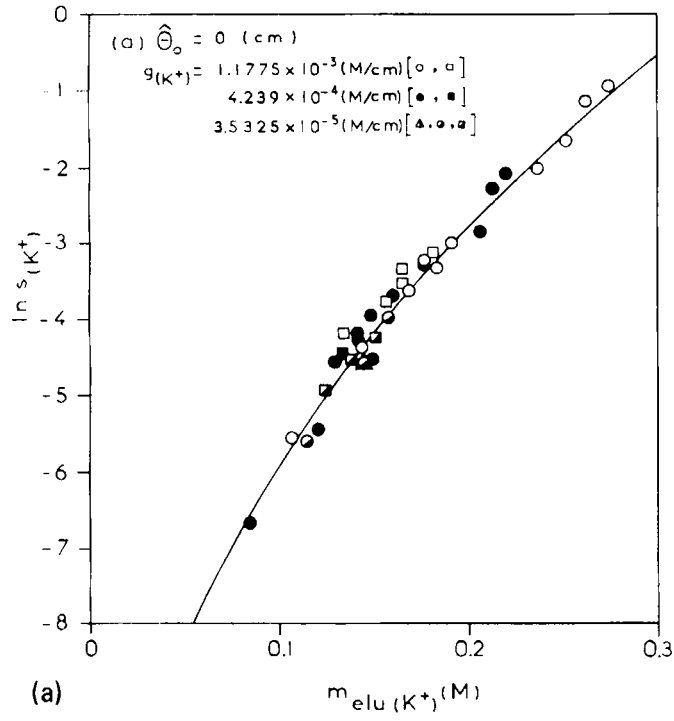

FIG. 3a. Points: Experimental plots of $\ln s_{(K+)}$ versus elution molarity, $m_{elu(K+)}$, at the center of gravity of lysozyme chromatographic peaks for three different slopes, $g_{(K+)}$, of the potassium gradient. It can be seen that all points are arranged making essentially a single array in spite of the three different $g_{(K+)}$'s that are applied. Curve: Theoretical curve calculated from Eq. (4) on the basis of the assumption of $\hat{\theta}_0 = 0$ cm, which is independent of the $g_{(K+)}$ value. It also is assumed $\varphi' = 9\,M^{-1}$, $x' = 7$, and $\ln q = 6.7$. (Reproduced, with modifications, from Fig. A2 in Ref. 2, Appendix II.)

the same as those assumed in both Figs. 1 and 2 with $g = 4.239 \times 10^{-4}$ M/cm and $m_{in} = 0.0015\,M$. The values of the experimental parameters that are used for the calculation of Fig. 4 are the same as in Fig. 2(c). Equation (18) shows that, if L tends to zero, then the chromatogram tends to an infinitesimal peak appearing at $m = m_{in}$. Figure 4 shows that, with an increase of L, the width in the chromatographic peak begins to increase. After the first increase, however, it decreases with an increase of L (see Fig. 4). It can be shown that the width in the peak again increases with an increase in L when L attains the order of magnitude of 50 cm. In both Refs. 2 and 5 the parallel conclusion has been obtained on the basis of the assumption of

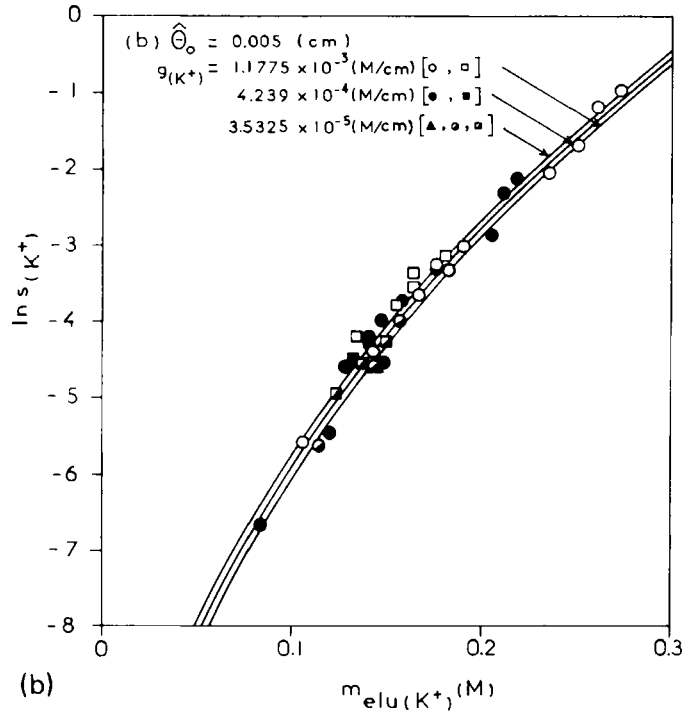

FIG. 3b: Points: As in Fig. 3a. Curves: Theoretical curves calculated from Eq. (18) assuming $\hat{\theta}_0 = 0.005$ cm. It also is assumed $\varphi' = 9\ M^{-1}$, $\theta_0 = 0.2$ cm, $x' = 7$, and $\ln q = 6.6$ (the same assumptions as those involved in Fig. 2 c). The curves are virtually independent of the θ_0 value, however.

the infinitesmal B-dif. plus STFH-dif. effect (see Figs. 1 and 2 in Ref. *2* and Fig. 1 in Ref. 5).

Remark. At the limit when L tends to $4\hat{\theta}_0$ (= 0.02 cm), the first and second equalities in Eq. (18) coincide with each other. From the structure of the second equality in Eq. (18), it can be understood that, when $L \leq 4\hat{\theta}_0$, then the total chromatogram, including the "sharp peak" occurring at $m = m_{in}$, can be calculated. In this instance, however, the "sharp peak" (at $m = m_{in}$) cannot practically be distinguished from the other part of the chromatogram, since the total chromatogram begins abruptly at $m = m_{in}$ and the height of it decreases monotonically with an increase of m when $m > m_{in}$ (see the pattern for $L = 0.02$ cm in Fig. 4). When $L > 4\hat{\theta}_0$, the chromatogram begins to migrate toward high m values with an increase of L (see Fig. 4). It can be assumed (see Theoretical Section B), however, that a part of the total chromatogram remains at molarity, $m = m_{in}$, of the ions forming a sharp

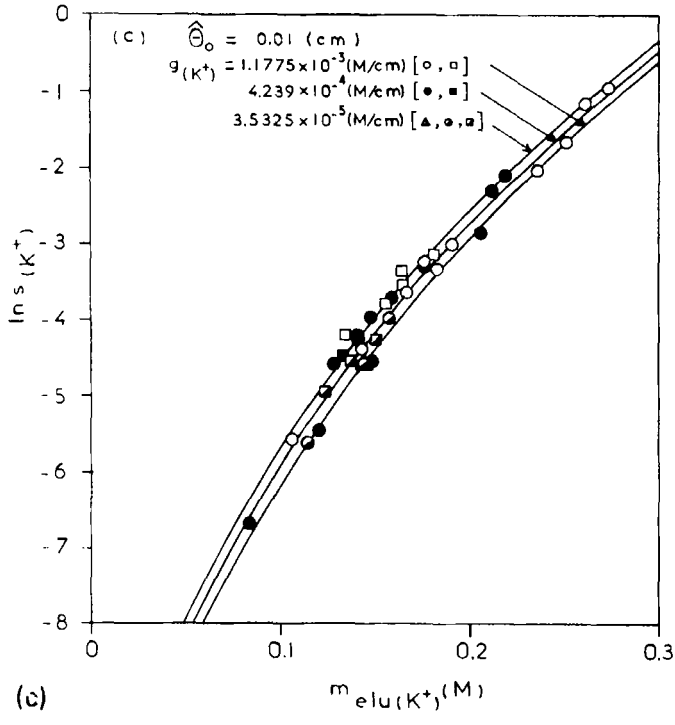

FIG. 3c: Points: As in Fig. 3a. Curves: As Fig. 3b but under the assumption of $\hat{\theta}_0 = 0.01$ cm; the other assumptions that are made are $\varphi' = 9\ M^{-1}$, $\theta_0 = 0.1$ cm, $x' = 7$, and $\ln q = 6.5$ (the same assumptions as those involved in Fig. 2 f). The curves are virtually independent of the θ_0 value, however. For details, see text.

peak. This peak gradually disappears with an increse in L (see below). In Fig. 4, only the part of the total chromatogram from which the sharp peak at $m = m_{in}$ is eliminated is shown. No detailed information on the shape of the sharp peak can be obtained from the present theory (see Ref. 5, Theoretical Section B). However, by measuring the area under a theoretical pattern in Fig. 4, the proportion of the actual chromatogram that should be occupied by the sharp peak at $m = m_{in}$ can be estimated. The smaller the area, the larger should be the proportion occupied by the peak. Thus Fig. 4 shows that this proportion decreases with a decrease in height in the theoretical pattern occurring at $m = m_{in}$. Therefore, it is only when L is smaller than, or of the order of magnitude of, 0.1 cm that the sharp peak should virtually appear in the actual chromatogram (see Fig. 4). When $L \gtrsim 1$ cm, the peak does not exist any more, and the chromatogram in Fig. 4 should virtually represent the total actual chromatogram.

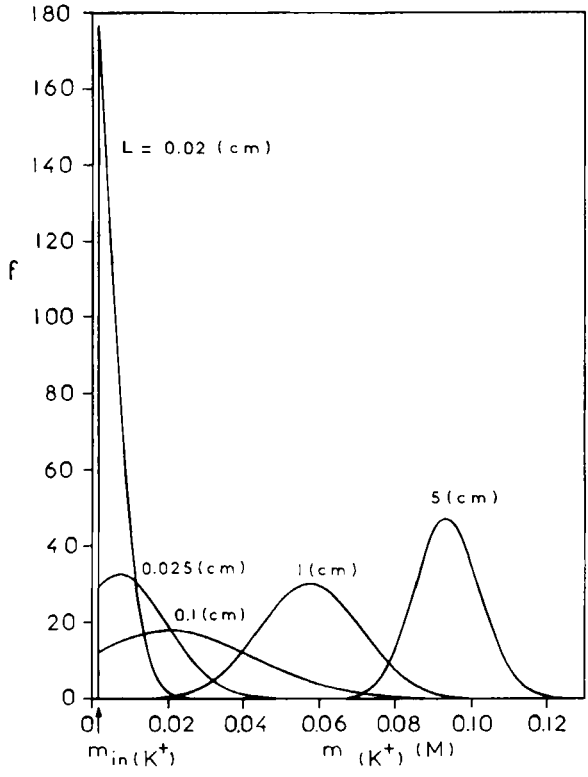

FIG. 4. Theoretical chromatograms for lysozyme on columns with several small lengths, L, calculated from Eq. (18); the sharp peak that should appear at $m = m_{in}$ is not illustrated except when $L = 4\theta_0 = 0.02$ cm. Except for the column length, the experimental conditions that are assumed are the same as those assumed in both Figs. 1 and 2 with $g_{(K^+)} = 4.239 \times 10^{-4} M/\text{cm}$ and $m_{in(K^+)} = 0.0015\ M$; the values of the experimental parameters that are used for the calculations are the same as in Fig. 2(c) with $\varphi' = 9\ M^{-1}$, $\theta_0 = 0.2$ cm, $\hat{\theta}_0 = 0.005$ cm, $x' = 7$, and $\ln q = 6.6$. For details, see text.

DISCUSSION

The thermal Brownian diffusion coefficient of lysozyme is about 1.1×10^{-6} cm^2/s (7). Assuming that the flow rate of the solvent on a HA column with a diameter of 1 cm is 0.5 mL/min (see Ref. *1*, Introduction Section), it can, therefore, be estimated that the contribution of the Brownian diffusion effect to the parameter $\hat{\theta}_0$ is about 10^{-4}cm. This is only about 2% of the maximum possible value, 0.005 cm, of $\hat{\theta}_0$ (see Some Numerical Calculations and the Relationship with the Experiment Section). Provided $\hat{\theta}_0 = 0.005$ cm, the effect of Brownian diffusion is therefore virtually negligible within the

total effect of B-dif. plus STFH-dif. If $\hat{\theta}_0$ is much smaller, the contribution of Brownian diffusions to the B-dif. plus STFH-dif. effect should be important. In this instance, however, the B-dif. plus STFH-dif. effect itself is negligible in comparison with the effect of diffusion due to the first type of flow heterogeneity. Therefore, at any rate, the effect of longitudinal Brownian diffusion should be negligible with HA chromatography. In Ref. *1* the assumption of a quasistatic chromatographic process was introduced with HA chromatography. This arises from the experimental fact that virtually no deformation of the chromatogram or the change in elution position occurs when the flow rate is changed (see Ref. *1*, Introduction Section). The conclusion derived above that the effect of longitudinal Brownian diffusion is negligible is consistent with the assumption of the quasi-static process. Since even the total effect of B-dif. plus STFH-dif. is small with $\hat{\theta}_0 \lesssim 0.005$ cm, the earlier theory (*1–5*) and several predictions made on the basis of that theory (*2, 4, 5*) can be considered to be valid from a practical point of view.

Since the total longitudinal diffusion on the column is essentially due to diffusion provoked by the first type of flow heterogeneity (see above), it can be expected that the chromatographic resolution will drastically increase if the effect of the first type of flow heterogeneity can be eliminated. In Ref. *6*, Theoretical Section D, it was mentioned that the first type of flow heterogeneity cannot be realized near the top of the column due to its mechanism. It can therefore be suggested that the effect of diffusion due to the first type of flow heterogeneity can be eliminated experimentally if a series of thin plates that are connected to one another by capillary tubes are used instead of a single column with the same total length. The chromatographic resolution might drastically increase.

APPENDIX

Here, a differential equation (Eq. 7) is derived from which Eq. (2) can be generated as a solution under the initial boundary condition given by Eq. (1). Equation (2) originally was derived as an approximate form of the solution (obtained under the boundary condition of Eq. 1) of the fundamental continuity equation of gradient chromatography [Eq. 17 in Ref. *3* (or Eq. 1 in Ref. 5); cf. Ref. *4*. This equation can be rewritten as

$$\mathrm{div}_m\left[\frac{\overrightarrow{1 - B(s, m)}}{B(s, m)} C - \frac{g\theta_0}{B(s, m)} \mathrm{grad}_m \frac{C}{B(s, m)}\right] + \frac{\partial C}{\partial s} = 0 \tag{A-1}$$

The approximation that has been used for the derivation of Eq. (2) from the

solution [Eqs. 62 and 73 in Ref. *3* (or Eqs. 12 and 6 in Ref. 5)] of Eq. (A-1) is that the molarity range over which a chromatogram appears is small around the mean elution molarity μ. This means (*4*) that the partition B_λ (Eq. 6) or B(Eq. A-1) of molecules in solution or the mobile phase is essentially constant within the band of molecules migrating on the column. This is essentially equal to the partition occurring, provided the molarity of the ions is μ. It can be considered that, if the same approximation is applied to Eq. (A-1) itself, the differential equation from which Eq. (2) can be generated as a solution can be derived. Thus, under this assumption, B in Eq. (A-1) should be a function of only s since B is a function of only μ (see above) and μ is a function of s (Eq. 4). Equation (A-1) should therefore be reduced into a form

$$g\theta_0\Phi(s)\frac{\partial^2 C}{\partial m^2} = \Psi(s)\frac{\partial C}{\partial m} + \frac{\partial C}{\partial s} \qquad \text{(A-2)}$$

The forms of both functions $\Phi(s)$ and $\Psi(s)$ will be determined below (1) by solving Eq. (A-2) under the boundary condition of Eq. (1), and (2) by comparing the solution with Eq. (2). However, let us first derive a solution of Eq. (A-2) under a more general boundary condition given by Eq. (8) or

$$C(s = +0, m) = C_0(m) \qquad \text{(A-3)}$$

where C_0 is any function. Thus, introducing Fourier transformations,

$$\mathcal{F}(C) = U(s, M) \equiv \frac{1}{\sqrt{2\pi}}\int_{-\infty}^{\infty} e^{-iMm}C(s, m)\,dm \qquad \text{(A-4)}$$

$$\mathcal{F}\left[\frac{\partial C}{\partial m}\right] = iMU(s, M) \qquad \text{(A-5)}$$

and

$$\mathcal{F}\left[\frac{\partial^2 C}{\partial m^2}\right] = -M^2U(s, M) \qquad \text{(A-6)}$$

Equation (A-2) is transformed into

$$-g\theta_0M^2\Phi(s)U = iM\Psi(s)\,U + \frac{\partial U}{\partial s} \qquad \text{(A-7)}$$

from which

$$U(s\ \ M) = F(M)e^{-\int_0^s |g\theta_0M^2\Phi(s)+iM\Psi(s)|ds} \qquad \text{(A-8)}$$

is obtained where F is any function. Since, on the other hand,

$$C_0(m) = \frac{1}{\sqrt{2\pi}} \int_{-\infty}^{\infty} e^{imM} U(0, M)\, dM = \frac{1}{\sqrt{2\pi}} \int_{\infty}^{\infty} e^{imM} F(M)\, dM \quad \text{(A-9)}$$

we have

$$F(M) = \frac{1}{\sqrt{2\pi}} \int_{-\infty}^{\infty} e^{-iMm'} C_0(m')\, dm' \quad \text{(A-10)}$$

which, with Eq. (A-8), leads to the final solution:

$$\begin{aligned} C(s, m) &= \frac{1}{\sqrt{2\pi}} \int_{-\infty}^{\infty} e^{imM} U(s, m)\, dM \\ &= \frac{1}{\sqrt{2\pi}} \int_{-\infty}^{\infty} C_0(m') \left\{ \frac{1}{\sqrt{2\pi}} \int_{-\infty}^{\infty} e^{-\int_0^s g\theta_0 M^2 \Phi(s)\, ds} \right. \\ &\qquad \left. e^{iM\left|m - \int_0^s \Psi(s)\, ds - m'\right|}\, dM \right\} dm' \\ &= \frac{1}{\sqrt{4\pi g\theta_0 \int_0^s \Phi(s)\, ds}} \int_{-\infty}^{\infty} C_0(m') e^{-\frac{\left|m - \int_0^s \Psi(s)\, ds - m'\right|^2}{4g\theta_0 \int_0^s \Phi(s)\, ds}} dm' \end{aligned} \quad \text{(A-11)}$$

For the derivation of the extreme right-hand side of Eq. (A-11), the fact that the total integral, $\oint e^{-z^2/2}\, dz$ (where $z = x + iy$), along the four sides of a rectangle on the complex xy-plane is zero has been utilized (Cauchy theorem). One of the sides of the rectangle coincides with the x-axis, and the rectangle is symmetrical around the y-axis. Especially when $C_0(m')$ is given by the delta function (Eq. 1) or when

$$C_0(m') = \delta(m' - m_{\text{in}}) \quad \text{(A-12)}$$

Eq. (A-11) reduces to

$$C(s, m) = \frac{1}{\sqrt{4\pi g\theta_0 \int_0^s \Phi(s)\, ds}} e^{-\frac{\left[m - \int_0^s \Psi(s)\, ds - m_{\text{in}}\right]^2}{4g\theta_0 \int_0^s \Phi(s)\, ds}} \quad \text{(A-13)}$$

Comparing Eq. (A-13) with Eq. (2),

$$\int_0^s \Psi(s)\, ds = \mu(s) - m_{in} \tag{A-14}$$

and

$$\int_0^s \Phi(s)\, ds = \frac{s}{[\bar{B}(s)]^2} \tag{A-15}$$

are obtained, from which

$$\Psi(s) = \frac{d\mu(s)}{ds} \tag{A-14'}$$

and

$$\Phi(s) = \frac{d}{ds}\left\{\frac{s}{[\bar{B}(s)]^2}\right\} \tag{A-15'}$$

are derived respectively.

We finally show that $d\mu(s)/ds$ (Eq. A-14') can be represented in terms of $\bar{B}(s)$ (see eq. 6) as

$$\frac{d\mu(s)}{ds} = \frac{1 - \bar{B}(s)}{\bar{B}(s)} \tag{A-16}$$

Thus, when $\theta_0 \rightarrow +0$, then Eq. (A-13) further reduces to

$$C(s, m) = \delta[m - \mu(s)] \tag{A-17}$$

(cf. Eq. A-14) showing that a sharp molecular band with infinitesimal width is formed at molarity:

$$\mu' = \mu(s) \tag{A-18}$$

On the other hand, μ' originally is defined by Eq. (A-23) in Ref. *1*, Appendix II, as

$$s = r(\mu') \equiv \int_{m_{in}}^{\mu'} \frac{B_\lambda(\mu'')}{1 - B_\lambda(\mu'')}\, d\mu'' \tag{A-19}$$

Equation (A-19) can also be derived from both Eqs. (4) and (6). Equations (A-18) and (A-19) show that

$$s = r[\mu(s)] \tag{A-20}$$

from which

$$1 = \frac{dr}{d\mu}\,\frac{d\mu}{ds} \tag{A-21}$$

is obtained. This leads to

$$\frac{d\mu(s)}{ds} = \frac{1}{dr/d\mu} = \frac{1 - B_\lambda[\mu(s)]}{B_\lambda[\mu(s)]} = \frac{1 - \bar{B}(s)}{\bar{B}(s)} \tag{A-22}$$

(cf. Eqs. A-19 and 6), which is Eq. (A-16) itself. Equation (A-16) can also be derived directly from Eqs. (4) and (6).

By substituting Eqs. (A-14′) and (A-15′) into Eq. (A-2), and taking into account Eq. (A-16), Eq. (7) can be obtained.

SYMBOLS

m mean molarity of competing ions in solution within the last infinitesimal vertical section at the bottom of the column, or the solution that has just been eluted out of the column. m increases linearly with increase in elution volume V with linear gradient chromatography. The chromatogram is represented as a function of m. In some instances, m also represents the mean ion molarity in solution within any vertical section of the column.

m_{in} initial molarity of competing ions at the beginning of the molarity gradient introduced at the top of the column.

L length of the column. In some instances, L also represents any longitudinal position on the column, i.e., the distance from the column top.

g positive constant representing the slope of the molarity gradient of competing ions in the column. This is expressed as an increase in mean ion molarity m (in solution within a column section) per unit column length, measured from the bottom to the top.

C and C' concentrations of sample molecules (under consideration) in a solution that has just been eluted out of the column. In some instances, C also represents the mean molecular concentration in solution within any vertical section of the column. C', as a function of m, represents a chromatogram.

f chromatogram, i.e., an expression of C' in which both parameters g and L are explicitly involved.

φ' positive constant characterizing the competing ion.

x' and q positive constants characterizing the sample molecule.

θ_0 positive constant with a dimension of length that measures the total longitudinal molecular diffusions in the column, i.e., diffusions due to the first and second types of flow heterogeneities and thermal Brownian diffusion.

$\hat{\theta}_0$ positive constant with a dimension of length that measures the longitudinal effect of B-dif. plus STFH-dif.

Acknowledgments

The author is grateful to Dr G. Bernardi for his interest in this work. The calculations were performed on CDC 6600 computer of the Faculty of Sciences, University of Paris.

REFERENCES

1. T. Kawasaki, *Sep. Sci. Techol., 16*, 325 (1981).
2. T. Kawasaki, *Ibid., 16*, 439 (1981).
3. T. Kawaskai, *Ibid., 16*, 817 (1981).
4. T. Kawasaki, *Ibid., 16*, 885 (1981).
5. T. Kawasaki, *Ibid., 17*, 319 (1982).
6. T. Kawasaki, "A theory of Stepwise Chromatography," *Ibid.*, In Press.
7. T. Imoto, L. N. Johnson, A. T. C. North, D. C. Phillips, and J. A. Pulpley, in *The Enzymes*, Vol. 7 (P. D. Boyer, ed.), Academic, New York, 1972, p. 665.

Received by editor March 2, 1981